



HAL
open science

Fracture rate dependency of an adhesive under dynamic loading

Noëlig Dagorn, Gérald Portemont, Vincent Joudon, Benjamin Bourel, Franck Lauro

► **To cite this version:**

Noëlig Dagorn, Gérald Portemont, Vincent Joudon, Benjamin Bourel, Franck Lauro. Fracture rate dependency of an adhesive under dynamic loading. *Engineering Fracture Mechanics*, 2020, 235, pp.107082. 10.1016/j.engfracmech.2020.107082 . hal-03186844

HAL Id: hal-03186844

<https://hal.science/hal-03186844>

Submitted on 18 May 2023

HAL is a multi-disciplinary open access archive for the deposit and dissemination of scientific research documents, whether they are published or not. The documents may come from teaching and research institutions in France or abroad, or from public or private research centers.

L'archive ouverte pluridisciplinaire **HAL**, est destinée au dépôt et à la diffusion de documents scientifiques de niveau recherche, publiés ou non, émanant des établissements d'enseignement et de recherche français ou étrangers, des laboratoires publics ou privés.

Fracture rate dependency of an adhesive under dynamic loadings

Noëlig Dagorn^{a,b,c,*}, Gérald Portemont^b, Vincent Joudon^a, Benjamin Bourel^c,
Franck Lauro^c

^a*Département Mécanique des Matériaux et Composites, Safran Aircraft Engines,
Rond-point René Ravaud - Réau, 77515 Moissy-Cramayel, France*

^b*DMAS, ONERA, F-59014 Lille, France*

^c*Laboratoire d'Automatique, de Mécanique et d'Informatique Industrielles et Humaines,
Université Polytechnique Hauts de France, Valenciennes, France*

Abstract

Adhesives joints are widely developed in aeronautic and automotive design applications. When subjected to impact loading, the rate sensitivity of adhesively bonded joints becomes a subject of interest. In this study, the mode I fracture behaviour of an aeronautic adhesive is characterized. Double Cantilever Beam tests are realized under different loading rates. A new protocol is developed to accurately measure the fracture toughness. The corrected beam theory with effective crack length is extended to measure the energy release rate during the crack growth stage. The main advantage of this new protocol is to accurately determine the crack speed without a direct experimental error. The validity of the analysis scheme is discussed considering dynamic effects. The crack speed measurement is validated by comparison to a conventional camera monitoring. The crack velocity is found to decrease with the crack length, while the fracture toughness remains unchanged.

Keywords: Adhesive fracture energy, Dynamic loading, Crack velocity, Beam Theory

*Corresponding Author

Email address: noelig.dagorn@gmail.com (Noëlig Dagorn)

Nomenclature

a	Crack length
a_0	Initial crack length
$a_{(\delta,P)}$	Effective crack length of the DCB specimen
\dot{a}	Crack velocity
$\dot{a}_{(\delta,G_m)}$	Crack velocity assuming a constant value G_m of the energy release rate
\ddot{a}	Crack acceleration
C	Compliance
E	Young modulus of the substrates
G	Energy release rate
G_c	Critical energy release rate
G_d	Dynamic energy release rate
G_m	Mean value of the energy release rate during the propagation stage
I	Substrate inertia moment
P	Load
b	Width of the DCB specimen
f_c	Cutoff frequency
h	Substrate thickness
u_0	Half the opening displacement δ
x	Distance from the loading axis
$u(x)$	Deflection of one beam of length a at a distance x
$\dot{u}(x)$	Deflection velocity
\dot{u}_0	Half the loading rate
U_{el}	Elastic energy
U_{kin}	Kinetic energy
V_{max}	Maximal crack velocity
W_{ext}	External work
δ	Opening displacement at the loading axis
$\dot{\delta}$	Opening displacement rate or loading rate
Δ	Crack length correction using the compliance
ρ	Substrates density

1. Introduction

Nowadays structural adhesive joints are widely used due to their advantages compared to mechanical joints. Indeed, adhesive joints present a more uniform stress distribution and a reduced weight. Load transmissions and stiffness are both improved, whereas rivets often present stress concentrations, which can affect the fatigue life. Adhesives are consequently an alternative more and more developed in the automotive and aeronautic industry. For instance, aeronautic fan blades can involve adhesively bonded joints. Due to its application, fan blades can be subject to bird strike. During a bird impact, crack propagation can occur in the adhesive layer, which is subjected to a wide range of loading rates. Thus, it is necessary to study the fracture behaviour of adhesives, particularly for different loading rates and during the crack propagation stage. The mode I critical energy release rate G_c of adhesives can be evaluated at the initiation stage under quasi-static loading using the standard Double Cantilever Beam test (DCB) [1][2]. However, there is no standard protocol for fracture toughness determination under dynamic loading nor during a crack propagation stage.

Multiple studies indicate a rate-dependency of the fracture toughness for different materials, such as epoxy resins [3] [4], carbon fibre reinforced polymers [5] [6] [7] or adhesively bonded joints [8] [9]. Moreover, the fracture behaviour can vary during the propagation stage, with a non-constant fracture toughness. A rising "R-curve" tendency at the beginning of the propagation is typically observed for laminated composite materials [10]. Besides, depending on the material and the geometry considered, the crack propagation can exhibit unstable ("stick-slip") or a stable continuous behaviour [11] [12]. The same material can exhibit both unstable and stable behaviour, depending on the loading rate [13]. Therefore, the single value of G_c at the initiation stage obtained with the standard protocols [1][2], is not always sufficient to accurately describe a crack advance. The crack propagation stage necessitates further understanding.

Crack propagation can be studied with a simple approach based on the notion of velocity. In the literature, the fracture toughness was found to depend upon the crack propagation velocity. For epoxy resins [4], a rising crack velocity implies a higher fracture toughness. Opposite tendencies can be found concerning the relation between the crack speed and the fracture toughness in composite laminates [9] [14]. For unstable crack propagation, a linear response of the crack velocity to the energy release rate was proposed for composite laminates [15]. This relation was inspired from the linear relationship between the dynamic stress intensity factor and the crack speed introduced by Ravi-Chandar [16]. However, various relationships are required to accurately describe the different loading rates. Indeed, for the same loading rate and same fracture toughness, a stiffer specimen exhibits a higher crack speed [9].

Thus, there is not a clear unique trend to accurately describe the coupling between crack velocity, loading rate and fracture toughness. Modelling this complex coupling is quite difficult because the experimental evaluation is a challenging issue. The fracture toughness determination is very sensitive to the accuracy of the crack length measurement. Due to its singularity, the crack tip position is intrinsically difficult to monitor. This issue has led many authors to use various experimental set up. A recent literature review reported the different protocols and analysis developed [17]. A conventional approach is to use a camera monitoring. Under a continuous loading, a camera with a high resolution can be used for the crack tip detection. For loading rate up to 30 m/s, a high speed camera is necessary to acquire the crack tip position with a sufficient frame-rate [7] [18]. Due to the high acquiring frequency, a lower spatial resolution has to be used, which can limit the crack length measurement with a delay on the real crack tip. Moreover, the definition of the crack tip depends on the experimenter's interpretation. To avoid the expensive use of high-speed cameras, others authors used the variation of electrical resistance to measure the crack length. The electrical resistance can be measured using conductive paint [19] or wires along the anticipated crack path [20]. The small electric sensitivity to the crack advance is sufficient for monitoring large structures but its accuracy on crack length measurement generates huge discrepancy on the fracture toughness determination. The crack tip position can also be triangulated using acoustic emission with the flying time difference between the sensors [21]. However, the resolution of this method is directly dependent of the size of the sensors used. All these developments show that the crack growth acquisition is very challenging. This explains why, according to the author's knowledge, few studies have been focused on the coupling relationship between the crack speed, the fracture toughness and the loading rate.

The aim of this paper is to present a new protocol, based on DCB tests, to accurately measure both the crack velocity and the fracture toughness, under several loading rates, in a structural adhesive joint. In the first section, the authors describe theoretical considerations on the protocol. The validity of the protocol is discussed considering dynamic effects due to the crack propagation and to the dynamic loading. In the second section, fracture tests under diverse loading rates are presented. The accuracy of the new protocol is experimentally demonstrated by comparison to a conventional tracking with a camera in section three. The final section shows that the specimen stiffness is a key parameter to describe the global coupling between the fracture toughness, the crack speed and the loading rate.

2. Theory

2.1. Static Analysis

In this section, a protocol is developed to measure both the fracture toughness and the crack velocity during a propagation stage. First of all, the energy

release rate G is expressed in the common form [22]

$$\frac{d(W_{ext} - U_{el} - U_{kin})}{bda} = G - \frac{dU_{kin}}{bda} \quad (1)$$

where W_{ext} is the external work, U_{el} is the elastic energy and U_{kin} is the kinetic energy. The crack is assumed to have a straight front of size b and an extension da of the crack length a . The kinetic term is often neglected in a static analysis. The energy stored in the adhesive is also negligible compared to the one stored in the substrates. These substrates are expected to have an elastic mechanical behaviour.

Equation (1) shows that the crack tip position must be known to evaluate the fracture toughness. The conventional method is to experimentally monitor the crack length. However, the crack tip position can also be expressed as a function of the compliance of the specimen with a beam theory. This concept of effective crack length was introduced by BRK Blackman et al. [23] on the mode II end-loaded split (ELS) test to calibrate the initial crack length a_0 before crack propagation. It was then applied on the mode I Double Cantilever Beam test [24] and widely developed for other pure and mixed-mode tests by MFSF De Moura et al. [25] [26] [27]. Indeed, considering the DCB test described in Figure 1 with two balanced arms of thickness h and of width b , the effective crack length can be obtained with the following equation :

$$a_{(\delta,P)} = \left(\frac{Ebh^3}{8} \right)^{1/3} \left(\frac{\delta}{P} \right)^{1/3} \quad (2)$$

Where E is the elastic modulus of the arms, P is the load applied to the arms and δ is the displacement at the loading axis. The new protocol consists in extending this Corrected Beam Theory with Effective crack length method (CBTE) to the crack propagation stage. Consequently, a crack length time history and crack velocity can be evaluated using equation (2).

Then the static energy release rate G becomes independent of the crack length :

$$G = \frac{3Eh^3\delta^2}{16a^4} = \frac{3}{2h} \left(\frac{8P^4\delta^2}{Eb^4} \right)^{1/3} \quad (3)$$

Therefore, the extended CBTE allows the dynamic acquisition of G and $a_{(\delta,P)}$ during a crack propagation stage, only using the load and the opening displacement. The experimental monitoring of the crack position is not necessary. Besides, assuming a constant mean value G_m of the energy release rate during the test, the crack position and velocity can also be derived from equation (3)

$$\dot{a}_{(\delta,G_m)} = \left(\frac{3Eh^3}{16G_m} \right)^{1/4} \frac{\dot{\delta}}{2\sqrt{\delta}} \quad (4)$$

which means for a constant fracture toughness the crack velocity is expected to diminish during a DCB test. Indeed despite a constant displacement rate $\dot{\delta}$ the crack velocity is not constant. Equation (4) demonstrates that the crack speed

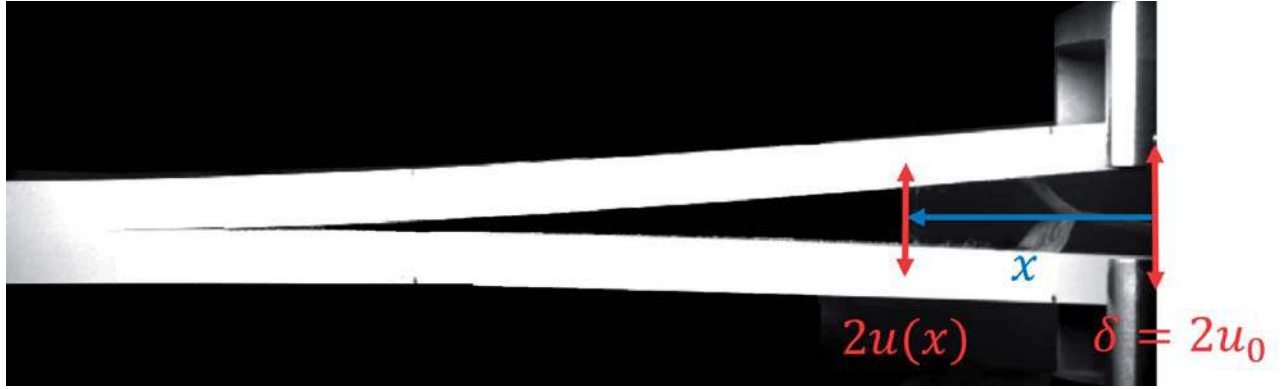


Figure 1: Double Cantilever Beam test

is sensitive to the geometry of the specimen and to the Young modulus of the substrates.

The extended CBTE gets the advantage that the effective crack length can be estimated without the experimental error, due to the images post treatment of the crack tip position, monitored with a camera. However some requirements have to be fulfilled to ensure its validity during a propagation stage and for dynamic loading rates.

2.2. Validity of the extended CBTE

The crack propagation stage is intrinsically a dynamic phenomena with creation of kinetic energy. Moreover a dynamic loading implies some kinetic energy in the substrates. These two phenomenon can be taken into account considering the kinetic term of equation (1). The dynamic energy release rate is then defined as

$$G_d = G - \frac{dU_{kin}}{bda} \quad (5)$$

The evaluation of the kinetic term can be quite difficult. BRK Blackman [13] presented a simplified way to take it into account. His method is detailed below. The "Berry Method" [28] assumes a static vertical displacement profile to approximate the deflexion u along the beam :

$$u(x) = u_0 \left(1 - \frac{3x}{2a} + \frac{x^3}{2a^3} \right) \quad (6)$$

where u_0 is the deflexion at the loading point and x is the distance from the load-line as described in Figure 1. The deflexion velocity \dot{u} is obtained by derivation of equation (6). An integration along the beam is used to compute the kinetic energy of one beam. This energy has to be doubled to model correctly the DCB test at every instant t with two built-in beams of length a .

$$U_{kin}(t) = 2 \frac{1}{2} \rho b h a(t) \int_{x=0}^a (\dot{u})^2 dx \quad (7)$$

$$U_{kin}(t) = \rho b h a \left(\frac{66\dot{u}_0^2}{280} + \frac{6u_0^2\dot{a}^2}{35a^2} + \frac{33u_0\dot{u}_0\dot{a}}{140a} \right) \quad (8)$$

Where ρ is the density of the substrates, \dot{u}_0 is half the loading rate and \dot{a} the crack velocity. Equation (8) takes into account the substrates kinetic energy, due both to dynamic loading rate through \dot{u}_0 , and to crack propagation through \dot{a} .

A first condition to fulfill is that the CBTE accurately describe the energy in the DCB specimen. Thus the kinetic energy equation (8) must be negligible compared to the elastic one that follows

$$U_{el} = \frac{3EI\delta^2}{4a^3} \quad (9)$$

Where I is the moment of inertia of a single arm.

The second condition to fulfill is that the kinetic term $\frac{dU_{kin}}{bda}$ is insignificant compared to the static measurement equation (3). From equation (8) the kinetic term can be calculated :

$$\frac{dU_{kin}}{bda} = \rho b h \left(\frac{66\dot{u}_0^2}{280} + \frac{6u_0^2(2\ddot{a} - \dot{a}^2)}{35a^2} + \frac{33u_0\dot{u}_0\ddot{a}}{140\dot{a}} \right) \quad (10)$$

with \ddot{a} the crack acceleration. Then the fracture toughness measurement can be considered only with the static value equation (3). If these two conditions are fulfilled, the determination of G_c is possible during a propagation stage and under dynamic loading.

In order to validate the extended CBTE, the authors choose to conduct Double Cantilever Beam tests. The fracture characterization of an adhesive is realized under several loading rates. The extended CBTE is applied and compared to the standard analysis [2].

3. Experiments

3.1. Sample preparation

The experimental investigation was performed on a viscoelastic-viscoplastic epoxy adhesive including a fiber polyamid support. The adhesive was provided by Safran Aircraft Engines. The adherends used in this study were high strength aluminum substrates (Al2024 T351), to avoid the plastic regime. The substrates were first prepared in a phosphoric anodic oxidation bath. An epoxy primer, provided by Solvay, was applied on the surfaces. According to the supplier requirements, the adhesive was cured between two sheets of aluminum at 150°C during 360 minutes at 350 kPa. The DCB specimens were then machined following the recommendations of the ASTM D3433 standard [1]. The specimens total length was of 350mm for quasi-static testing. A lower length of 200mm was chosen for dynamic loading rates in order to limit the inertia of the specimen. The adhesive thickness was controlled every 10mm along each specimen, using a digital microscope Hirox RH-2000. For each specimen, the thickness standard deviation was always less than $70\mu m$ along the sample. An average thickness of $291 \pm 36\mu m$ on all the tested specimens was found.

The initial crack length was created by inserting a non-adherend teflon-made film of $40\mu\text{m}$ of thickness between the adhesive and the sheet of aluminum. Thus the crack initiates directly from the tip of the film. Specimens are first precracked using a tensile-testing machine Instron 4302 at a constant displacement rate of $5\text{mm}/\text{min}$. The opening displacement is stopped when the first drop in the load measurement is observed. The crack tip position before testing is measured using a digital microscope Hirox RH-2000 as shown in Figure 2. A white zone of around $20\mu\text{m}$ can be observed along the crack path.



Figure 2: Crack tip observation after the precracking operation in the joint using a microscope Hirox RH-2000

As shown in Figure 1, one side of the specimens was painted in white to improve the crack tip detection with a camera monitoring. The crack tip position monitoring has been performed in order to compare the obtained position with the one evaluated with the extended CBTE.

3.2. Testing

All specimens were tested under ambient conditions at a constant displacement rate. Four loading rates varying from 0.5 to $5000\text{mm}/\text{min}$ were considered. The experimental set-up is described Figure 3. The experimental investigation was performed with a high speed hydraulic machine Instron VHS. The displacement was imposed to the upper holder until final failure of the specimen. The opening displacement in the loading axis direction was recorded using an optical extensometer Zimmer 200-XH, with a measurement range of 20mm . The displacement measurement uncertainty was $40\mu\text{m}$. The load was recorded with a device resolution of $0,01\text{N}$ using a piezoelectric load cell Kistler 9031. This load cell was fixed to the lower holder. One side of the DCB specimen was monitored with a camera. A pixel resolution of around 0.15mm over a window of 896×312 pixels was considered. A high acquiring frequency was achieved with a Photron SA-X camera coupled with a Dewetron system, except for $\dot{\delta} = 0.5\text{mm}/\text{min}$. Due to technical issues, a DeweSoft camera GiGe-300 was used the quasi-static tests at $\dot{\delta} = 0.5\text{mm}/\text{min}$, with the same spatial resolution. A MATLAB code was created for the crack tip detection. A threshold criterion based on the relative pixel intensity was used for the crack tip detection. The number of tested specimens are detailed for each loading rate in Table 1.

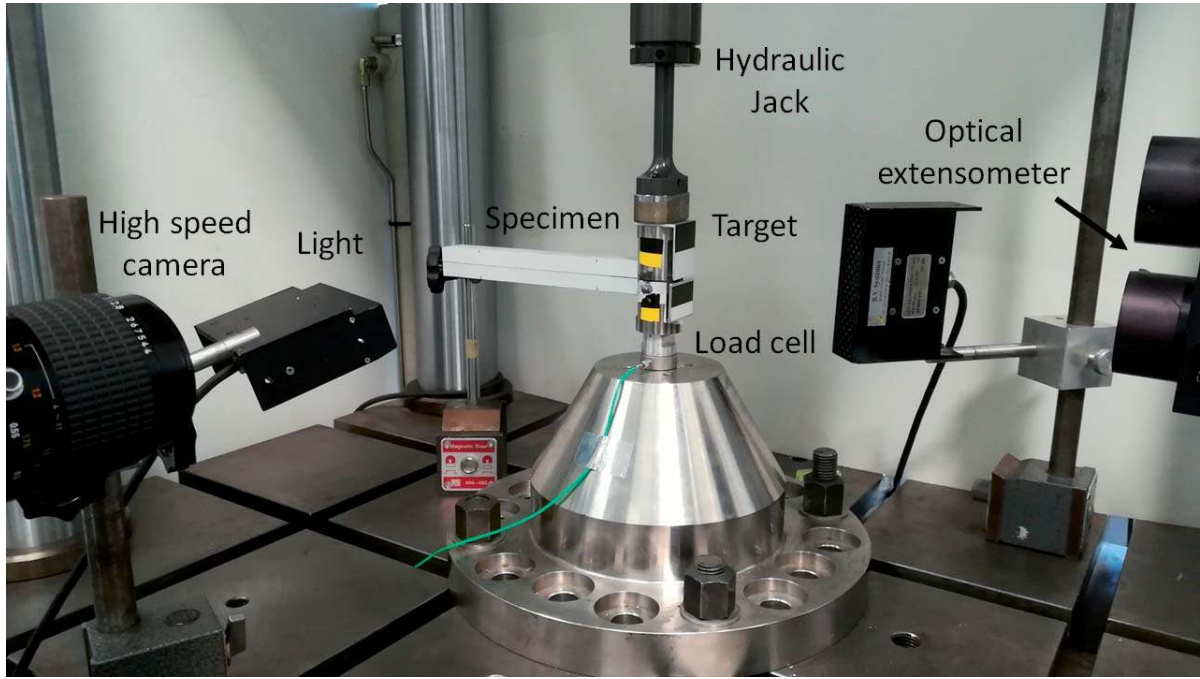


Figure 3: Experimental set up

δ (mm/min)	0.5	50	500	5000
Samples	3	5	3	2
Camera frame rate (fps)	1	125	1500	12500
Displacement/Load acquisition frequency (Hz)	10	1250	15000	125000

Table 1: Summary of the testing conditions

For each loading rate, one experimental load-displacement curve is plotted in Figure 4.

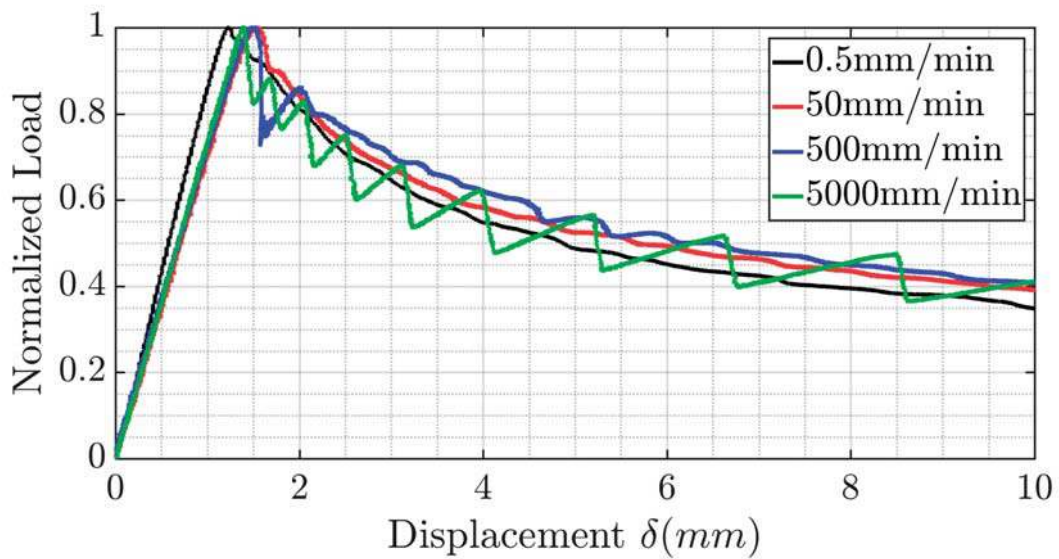


Figure 4: Load-Displacement curves for different loading rates

The slope of the elastic linear behaviour before crack propagation depends on the length of the precrack and is not analysed. The Load-displacement behaviour exhibits a low sensitivity to the loading rate up to 500mm/min. For the highest loading rate $\dot{\delta}=5000\text{mm}/\text{min}$, unstable "stick-slip" crack growth occurred with important drops in the load time history, as shown in Figure 5a. The unstable crack growth induced some vibrations in the specimen. These vibrations were directly observable on the load time history (see Figure 5b). A 1 ms mean local filter was applied for comparison with the lower loading rates. Despite a change of rupture mechanism, the load peak values are consistent with the other tests. The change of propagation behaviour from stable to unstable with the loading rate has already been observed for composite laminates [9].

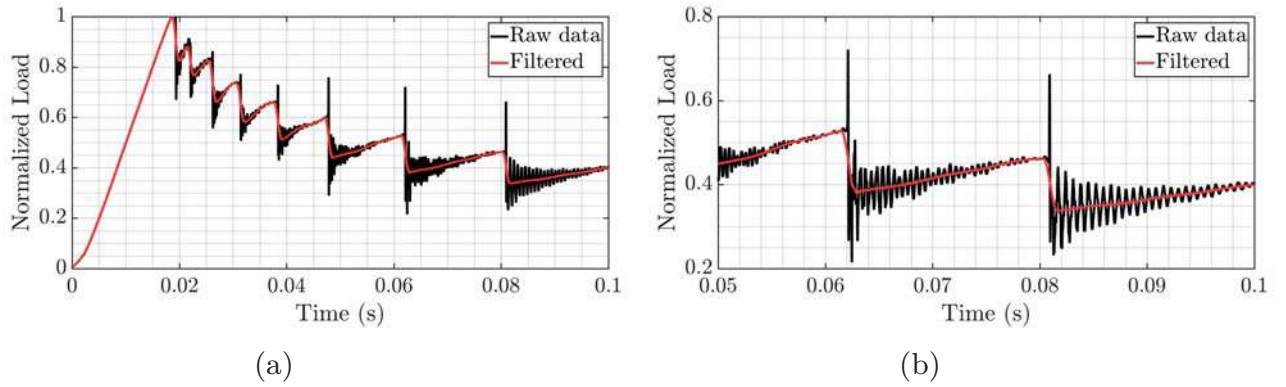


Figure 5: (a) Load-Displacement curve for $\dot{\delta} = 5000\text{mm}/\text{min}$. (b) Effect of the mean local filter on the signal

3.3. Fractography

After complete failure, the substrates were visually controlled and no sign of plasticity was observed. For all tested specimens the failure was cohesive. The same fracture surface was observed for specimens tested in the $\dot{\delta}$ range from 0.5 to 500mm/min. Specimens tested above $\dot{\delta}=500\text{mm}/\text{min}$ exhibit a different fracture surface. Figure 6 shows a comparison of the fracture surfaces between a steady-state propagation and a "stick-slip" behaviour.



Figure 6: Crack surfaces : 1 not bonded zone, 2 precrack, 3 crack propagation, 4 total failure of sample

Four zones can be observed. In zone 1, no adhesive was applied. A teflon insert was placed to ensure there was no bonding. This teflon film was removed after testing. Zone 2 and 4 correspond to unstable crack growth with a darker zone than for the steady-state crack propagation stage zone 3. Indeed, zone 2 corresponds to the pre-cracked zone. Zone 4 can be attributed to a final unstable failure of the specimen. Concerning the highest loading rate $\dot{\delta}=5000\text{mm}/\text{min}$, white crack arrest lines are observable on the fracture surface. The number of crack arrests lines corresponds to the number of drops in the load time history. Zone 3 was also observed using a microscope. Micrographics are plotted Figure 7. For a steady-state propagation, some initiation marks from the support are present while the "stick-slip" surface seems more homogeneous. The authors suggest one way to consider these fracture surfaces. For a steady-state propagation, the rupture could first occur at the interface between the support and the epoxy adhesive, before a failure in the epoxy adhesive. For high loading rates, the absence of marks suggests a simultaneous failure at the interface and in the epoxy adhesive. The absence of marks and the darker fracture surface suggests a more fragile failure behaviour, with a limited plasticity.

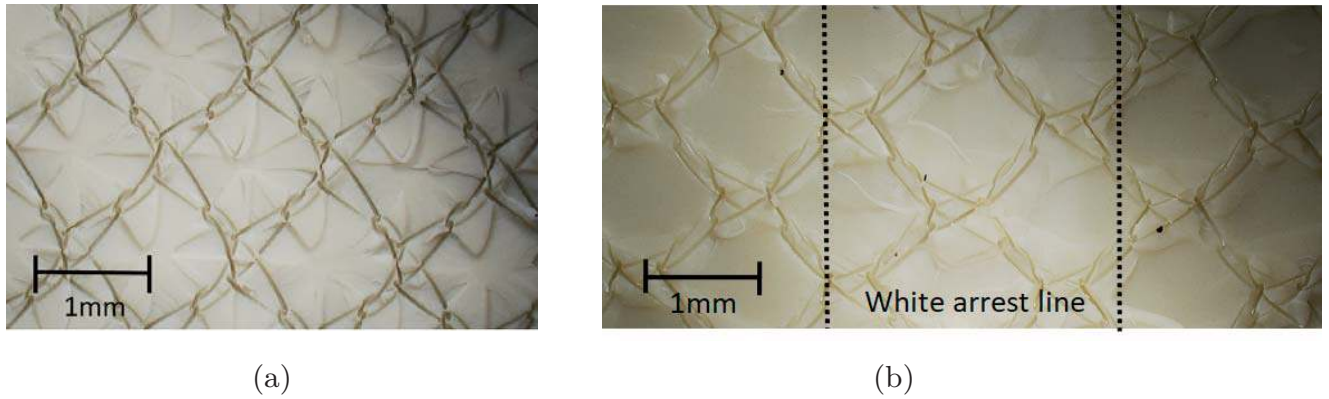


Figure 7: Post mortem microscopic view of the crack surface for (a) steady-state propagation and (b) "stick-slip" mechanism

For $\dot{\delta}=5000\text{mm}/\text{min}$ the observed vibrations during the test are not taken into account in the CBTE analysis. Consequently, only the specimens tested under a lower loading rate will be considered for measuring the crack speed.

4. Validation of the extended CBTE

The extended CBTE previously presented in section 2 was applied to evaluate the crack length according to equation (2). During the stable propagation stage and for all specimens tested, the measured maximal ratio between the kinetic energy (8) and the elastic energy (9) was 3.8%. The kinetic term was calculated according to equation (10) and was always less than 0.2% of the static value (3). Thus, the dynamic effects are neglected and the two conditions introduced in section 2.2 are fulfilled. The extended CBTE can be considered valid.

In the following, this method is compared to the standard Corrected Beam Theory (CBT) [2], which necessitates the crack length monitoring. The crack length measurement using the camera monitoring and the evaluated one using the extended CBTE are plotted Figure 8. An onset of crack length during all the test can be observed between the two methods.

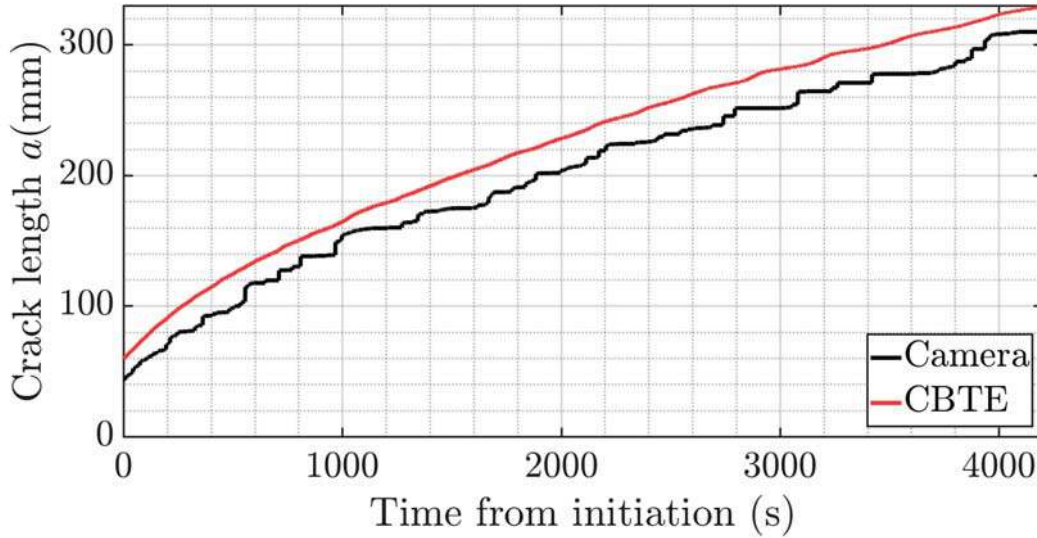


Figure 8: Comparison of the measured crack length using the extended CBTE and the camera monitoring for a test performed with $\dot{\delta}=0.5\text{mm}/\text{min}$

The standard CBT is not meant to be used for a crack propagation stage analysis. Indeed, only the onset of crack propagation is used in the standard. However, in order to observe the whole specimen, the field of the camera must be large. It leads to a low spatial resolution of around 0,15 mm. Consequently, a crack opening of less than 0,15 mm can not be detected by the camera. This opening represents half the thickness of the adhesive, so the crack tip measurement is obviously underestimated. Due to their high thickness of 12mm, the substrates have a high radius of curvature. This high radius makes the crack tip position even more underestimated. Moreover, the effective crack length does not coincide with the crack tip. It corresponds more to the built-in point in the DCB specimen with a zero opening. Therefore the effective crack length is meant to be greater than the crack tip experimentally observed. Using the measured crack length and the standard CBT protocol [2], the energy release rate can be evaluated using the following equation :

$$G = \frac{3P\delta}{2b(a + \Delta)} \quad (11)$$

Where Δ corresponds to a crack length correction for a beam which is not perfectly built-in. Δ is experimentally obtained from the Compliance-Crack length curve. The energy release rate using the CBT and the extended CBTE are plotted Figure 9. The crack length underestimated using the camera results in an overestimated energy release rate. According to equation (11), when the

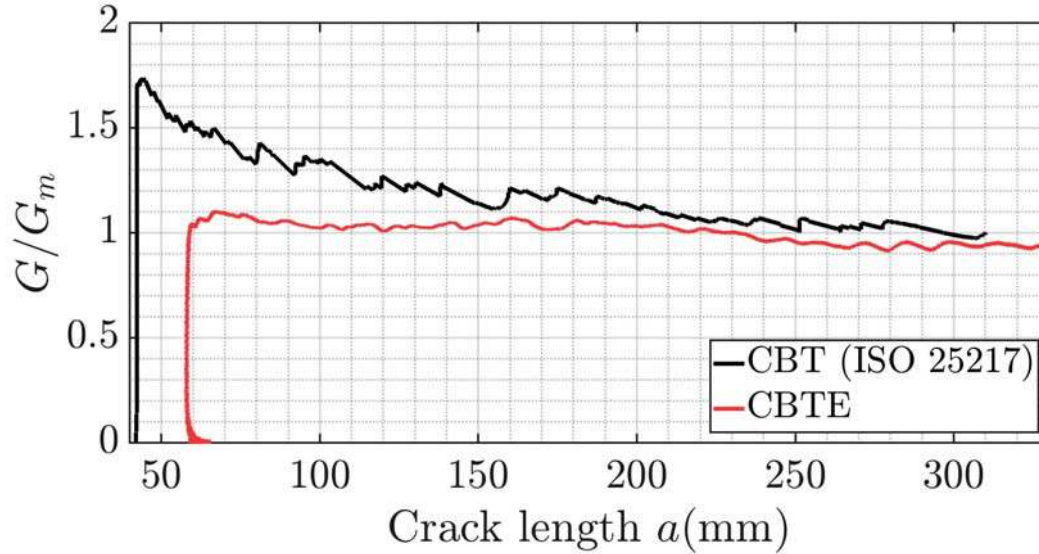


Figure 9: Comparison of the energy release rate using the extended CBTE and the standard CBT for a test performed with $\dot{\delta}=0.5\text{mm/min}$

crack grows the relative error diminishes. Therefore, the overestimated energy release rate, using the CBT, decreases until a plateau is reached. This plateau can be observed in Figure 9 for a crack length greater than 200mm. In order to reach this plateau, a sample longer than 200mm is necessary. On the contrary, the energy release rate remains quite constant in the propagation stage using the extended CBTE analysis. Thus, a short sample is sufficient to determine the fracture toughness.

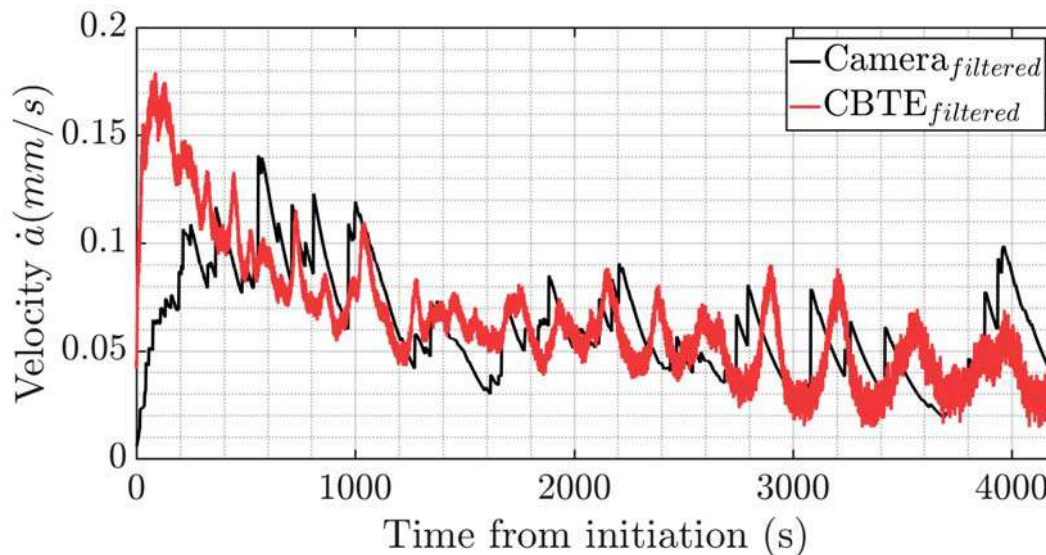


Figure 10: Crack velocity time history using the CBTE analysis and a camera for the monitoring of the crack tip position, for a test performed with $\dot{\delta}=0.5\text{mm/min}$

Besides, the crack velocities can be obtained using a derivative of the crack length and applying a low pass filter. The cutoff frequency f_c was defined using

the initial crack length a_0 and the maximal observed crack velocity V_{max} as follows

$$f_c = 2 \frac{V_{max}}{a_0} \quad (12)$$

The crack velocities experimentally obtained with the crack tip monitoring and the extended CBTE are plotted in Figure 10 for $\dot{\delta} = 0,5$ mm/min. According to equation (4), even if a constant critical energy release rate G is observed, the crack velocity is expected to diminish. This is consistent with the experimental results. The same decreasing crack speed during a DCB test was observed for a carbon/epoxy composite laminate [14]. Despite the onset of crack length measured between the CBTE and the camera, the crack velocities using the two methods coincide well. This good consistency confirms the application of the extended CBTE to determine the fracture toughness. Thus, only the extended CBTE analysis is considered in the next section.

5. Results and discussion

5.1. Rate dependency of G_c

For each loading rate, an R-curve is plotted in Figure 11. The initial crack length depends on the precrack. A larger R-curve was obtained for $\dot{\delta} = 0,5$ mm/min because of the larger length of the specimen. The energy release rate exhibits a loading rate dependency over five decades from 0.5 to 5000 mm/min.

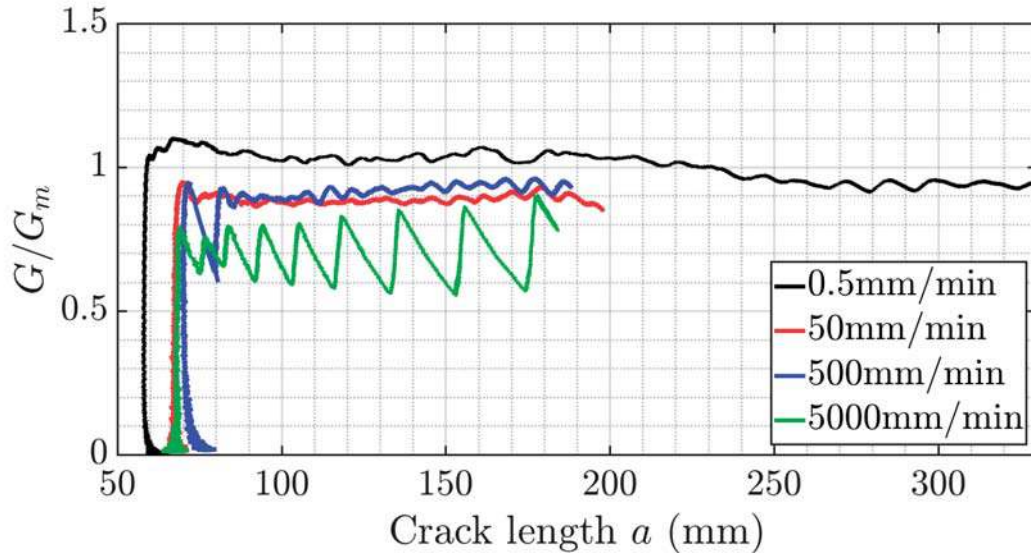


Figure 11: Normalized R-curve for different loading rates : Energy release rate using the CBTE analysis

For each specimen, an average energy release rate was determined over the whole propagation stage. For $\dot{\delta}=5000$ mm/min, only the initiation peak values were considered. For each loading rate, a mean fracture toughness and a

standard deviation were evaluated over the set of specimens. The mean fracture toughness values and standard deviations are summarized in Table 2. A decrease of 20% is coherent with the assumed limited plasticity under high loading rate. Indeed, a limited plasticity implies less energy dissipated in the fracture process zone.

$\dot{\delta}$ (mm/min)	0.5	50	500	5000
$\langle G \rangle / G_m$	1	0.918	0.925	0.818
$std(G) / G_m$ (%)	1.8	6.6	1.4	0.7

Table 2: Summary of the normalized measured fracture toughness over five decades of loading rate

5.2. Crack velocity

In the first section, the authors assumed a constant value of G during the propagation stage. According to the Figure 11, this assumption can be considered valid. The crack velocity can be modelled with a constant G value using equation (4). For a specimen tested with $\dot{\delta} = 0,5$ mm/min, the crack velocity time history experimentally obtained using the extended CBTE, and the ones calculated using equation (4) with different G values are plotted in Figure 12. Using the average value of G_m is efficient enough to describe the global crack speed decreasing. Therefore, there can be a whole range of crack speed for one single value of G_c and one unique loading rate $\dot{\delta}$. Besides, the crack velocity exhibits some oscillations.

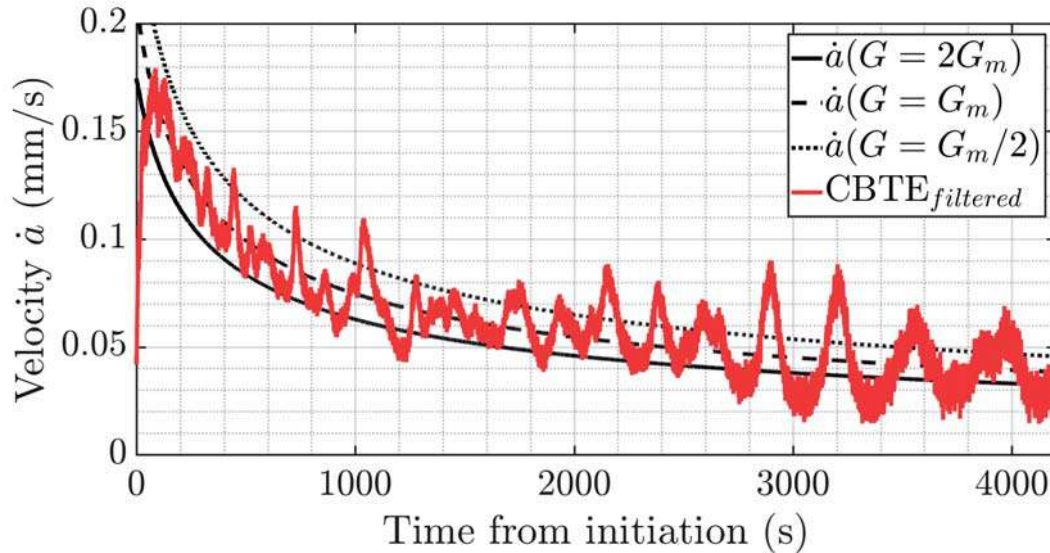


Figure 12: Crack velocity time history for $\dot{\delta}=0.5$ mm/min. Black lines assume a constant value of the energy release rate.

According to Figure 12, it should take a material dispersion of G_c from $G_m/2$ to $2G_m$ in order to explain the fluctuations of the crack velocity. This

dispersion is unlikely. The dependence of the ratio $\dot{a}/\dot{\delta}$ to the crack length is plotted for different loading rates in Figure 13. The amplitude of the crack speed oscillations rises with the loading rate. This rising tendency suggests there is a smooth transition over five decades of loading rate from the steady-state to the unstable crack growth.

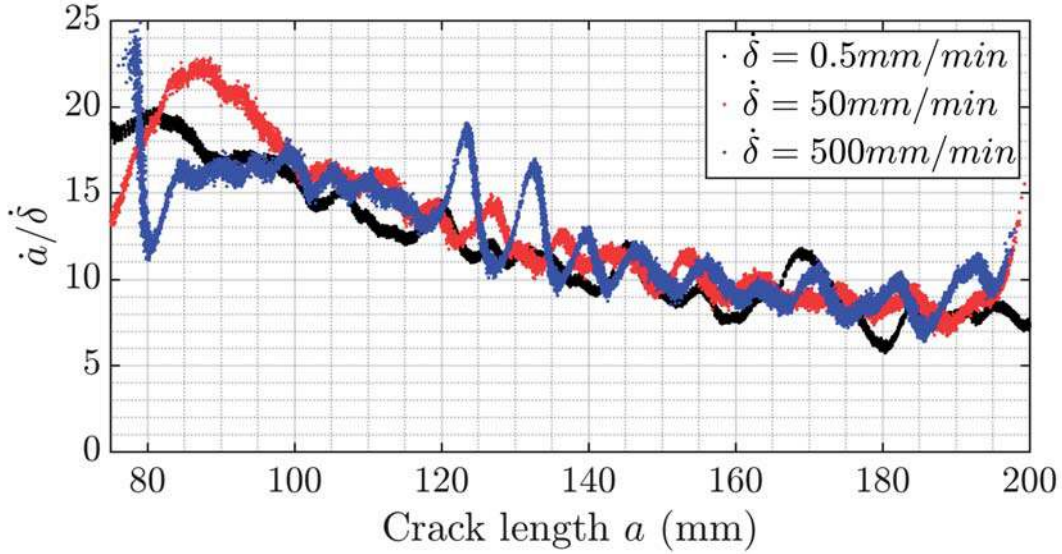


Figure 13: Ratio between crack velocity and loading rate, during the propagation stage, for different loading rates

The authors present two physical reasons to explain these oscillations. First, it is possible to consider that a crack propagation is an intrinsic transient mechanism. The crack growth would consist in a relaxation phenomenon, with a rising velocity stage and a decreasing velocity stage. In the rising stage, the potential energy exceeds the fracture toughness. Some kinetic energy is created. This kinetic energy is expressed through a crack acceleration. Once the potential energy is lower than the fracture toughness, the kinetic energy is consumed to balance the equilibrium. The crack decelerates to a new equilibrium position. However, this scheme seems unlikely. Indeed, the kinetic energy equation (8) was never significant compared to the elastic one equation (9).

A second mechanism could be an oscillation of the size of the fracture process zone. One should remember that the CBTE allows to measure the position $a_{(\delta,P)}$ of the built-in point with a zero opening in the DCB specimen. This position is beyond the real crack tip. The delay between the real crack tip and the built-in point corresponds to the approximate size of the process zone. Once $G = G_c$, the real crack tip and the built-in point move to a new equilibrium position. The new process zone is expected to be smaller for the crack to be stable. For a higher loading rate, a limited plasticity would induce a smaller size of the new process zone. Then, a new loading stage happens. During this loading stage the process zone has to grow. Thus, $a_{(\delta,P)}$ grows softly to a new position while the real crack tip sticks to its position. This scheme would result in an oscillating

crack velocity. A higher loading rate would induce bigger oscillations, until a macroscopic unstable crack growth behaviour is observed on the load time history for $\dot{\delta} = 5000$ mm/min.

6. Conclusion

In this work, the failure loading rate-dependency of an epoxy adhesive joint was studied. For that purpose, the Double Cantilever Beam test was considered under dynamic loading. A specific analysis protocol was developed to measure the fracture toughness. The analytical Corrected Beam Theory with Effective crack length method CBTE was extended to the stable crack propagation stage. This new protocol allowed to measure the crack tip position, the crack velocity and the fracture toughness using only the load and the opening displacement. The kinetic effects, due both to crack growth and to dynamic loading rates, were determined. This method was applied to DCB tests in the $\dot{\delta}$ range from 0,5 to 5000mm/min. Kinetic effects were quantified and considered negligible. For a steady-state propagation, the extended CBTE was compared to a conventional crack tip tracking with a camera. The new protocol was found more reliable since it avoids the experimental measurement error on the crack length.

Another key aspect of the extended CBTE, was the possibility to study the crack speed evolution during the propagation stage. It was found to decrease despite a constant fracture toughness. The beam theory was proved sufficient to describe the global coupling between the crack velocity, the fracture toughness and the loading rate. However, the fracture toughness experimental dispersion could not explain some oscillations of the crack speed. The amplitude of these oscillations rised with the loading rate, until a macroscopic unstable crack growth behaviour was observed for $\dot{\delta} = 5000$ mm/min. The unstable behaviour consisted in important drops on the load time history and visible crack arrest lines on the fracture surfaces. However, the decreasing fracture toughness and the rising amplitude of the crack velocity oscillations suggested a more progressive transition over five decades of increasing loading rate, from ductile to brittle failure, and consequently, from stable to unstable behaviour.

Further investigation could be made to acquire the crack tip velocity using a microscope at low loading rates, to confirm the crack speed oscillations. The dynamic acquisition of the size of the white plastic zone near the crack tip could bring more information about fracture process transition from stable to unstable crack growth.

7. Acknowledgements

The authors wish to thank the french national research program PRC MECA-COMP, and the french national research union ANRT, for their financial support, which enabled this study.

8. Bibliography

- [1] ASTM. D3433. *Standard Test Method for Fracture Strength in Cleavage of Adhesives in Bonded Metal Joints*, 2012.
- [2] ISO 25217. Adhesives. *Determination of the mode I adhesive fracture energy of structural adhesive joints using double cantilever beam and tapered double beam specimens*, 2009.
- [3] Chaosuan Kanchanomai, Suparat Rattananon, and M Soni. Effects of loading rate on fracture behavior and mechanism of thermoset epoxy resin. *Polymer Testing*, 24(7):886–892, 2005.
- [4] V Joudon, G Portemont, F Lauro, and B Bennani. Experimental procedure to characterize the mode I dynamic fracture toughness of advanced epoxy resins. *Engineering Fracture Mechanics*, 126:166–177, 2014.
- [5] Takayuki Kusaka, Masaki Hojo, Yiu-Wing Mai, Tomoaki Kurokawa, Take-toshi Nojima, and Shojiro Ochiai. Rate dependence of mode I fracture behaviour in carbon-fibre/epoxy composite laminates. *Composites Science and Technology*, 58(3-4):591–602, 1998.
- [6] S Mall, GE Law, and M Katouzian. Loading rate effect on interlaminar fracture toughness of a thermoplastic composite. *Journal of composite materials*, 21(6):569–579, 1987.
- [7] Huifang Liu, Hailiang Nie, Chao Zhang, and Yulong Li. Loading rate dependency of mode I interlaminar fracture toughness for unidirectional composite laminates. *Composites Science and Technology*, 167:215–223, 2018.
- [8] Michael May, Olaf Hesebeck, Stephan Marzi, Wolfgang Böhme, Jörg Lienhard, Sebastian Kilchert, Markus Brede, and Stefan Hiermaier. Rate dependent behavior of crash-optimized adhesives—experimental characterization, model development, and simulation. *Engineering Fracture Mechanics*, 133:112–137, 2015.
- [9] BRK Blackman, AJ Kinloch, FS Rodriguez Sanchez, WS Teo, and JG Williams. The fracture behaviour of structural adhesives under high rates of testing. *Engineering Fracture Mechanics*, 76(18):2868–2889, 2009.
- [10] S Hashemi, AJ Kinloch, and JG Williams. The effects of geometry, rate and temperature on the mode I, mode II and mixed-mode I/II interlaminar fracture of carbon-fibre/poly (ether-ether ketone) composites. *Journal of Composite Materials*, 24(9):918–956, 1990.
- [11] JW Gillespie Jr, Leif A Carlsson, and Anthony J Smiley. Rate-dependent mode I interlaminar crack growth mechanisms in graphite/epoxy and graphite/peek. *Composites Science and Technology*, 28(1):1–15, 1987.

- [12] AJ Smiley and RB Pipes. Rate effects on mode I interlaminar fracture toughness in composite materials. *Journal of composite materials*, 21(7):670–687, 1987.
- [13] BRK Blackman, JP Dear, AJ Kinloch, H MacGillivray, Y Wang, JG Williams, and P Yayla. The failure of fibre composites and adhesively bonded fibre composites under high rates of test. *Journal of Materials Science*, 31(17):4467–4477, 1996.
- [14] Hee You and Young-Jin Yum. Loading rate effect on mode I interlaminar fracture of carbon/epoxy composite. *Journal of reinforced plastics and composites*, 16(6):537–549, 1997.
- [15] Y Liu, FP van der Meer, and LJ Sluys. Cohesive zone and interfacial thick level set modeling of the dynamic double cantilever beam test of composite laminate. *Theoretical and Applied Fracture Mechanics*, 96:617–630, 2018.
- [16] Krishnaswamy Ravi-Chandar. *Dynamic fracture*. Elsevier, 2004.
- [17] Michael May. Measuring the rate-dependent mode I fracture toughness of composites– a review. *Composites Part A: Applied Science and Manufacturing*, 81:1–12, 2016.
- [18] Solver I Thorsson, Anthony Waas, Joseph Schaefer, Brian Justusson, and Salvatore Liguore. Effects of elevated loading rates on mode I fracture of composites laminates using a modified wedge-insert fracture method. *Composite Science and Technology*, 156:39–47, 2018.
- [19] Gershon Yaniv and Isaac M Daniel. Height-tapered double cantilever beam specimen for study of rate effects on fracture toughness of composites. In *Composite materials: testing and design (Eighth Conference)*. ASTM international, 1988.
- [20] C Guo and CT Sun. Dynamic mode-I crack-propagation in a carbon/epoxy composite. *Composite Science and Technology*, 58(9):1405–1410, 1998.
- [21] Mark Jonathan Eaton, Rhys Pullin, and Karen Margaret Holford. Acoustic emission source location in composite materials using delta t mapping. *Composites Part A: Applied Science and Manufacturing*, 43(6):856–863, 2012.
- [22] S Hashemi, A J Kinloch, and J M Williams. The analysis of interlaminar fracture in uniaxial fibre-polymer composites. *Proc. R. Soc. Lond. A*, 427(1872):173–199, 1990.
- [23] BRK Blackman, AJ Kinloch, and M Paraschi. The determination of the mode II adhesive fracture resistance, G_{IIc} , of structural adhesive joints: an effective crack length approach. 72(6):877–897, 2005.

- [24] BRK Blackman and J Williams. Crack length determination difficulties in composites-their effect on toughness evaluation. International conference on fracture ICF, 2005.
- [25] MFSF De Moura, RDSG Campilho, and JPM Gonçalves. Pure mode II fracture characterization of composite bonded joints. *International Journal of Solids and Structures*, 46(6):1589–1595, 2009.
- [26] MFSF De Moura, N Dourado, and J Morais. Crack equivalent based method applied to wood fracture characterization using the single edge notched-three point bending test. *Engineering Fracture Mechanics*, 77(3):510–520, 2010.
- [27] MFSF De Moura, JMQ Oliveira, JJJ Morais, and J Wavier. Mixed-mode I/II wood fracture characterization using the mixed-mode bending test. *Engineering Fracture Mechanics*, 77(1):144–152, 2010.
- [28] JP Berry. Some kinetic considerations of the griffith criterion for fracture-I: Equations of motion at constant force. *Journal of the Mechanics and Physics of Solids*, 8(3):207–216, 1960.